PERGAMON

Renewable and Sustainable Energy Reviews
5 (2001) 1–37

RENEWABLE
& SUSTAINABLE
ENERGY REVIEWS

www.elsevier.com/locate/rser

Adsorption refrigeration research in Shanghai Jiao Tong University

R.Z. Wang *

Institute of Refrigeration and Cryogenics, Shanghai Jiao Tong University, Shanghai 200030, China

Received 20 April 2000; received in revised form 10 July 2000; accepted 31 July 2000

Abstract

The research work on adsorption refrigeration in Shanghai Jiao Tong University (SJTU) started in 1993, various adsorption refrigeration cycles have been investigated, such as continuous heat recovery cycle, mass recovery cycle, thermal wave cycle, convective thermal wave cycle, cascade multi effect cycle, hybrid heating and cooling cycle etc. Several prototype adsorption refrigeration systems have been developed and tested, typical examples are continuous heat regenerative adsorption ice maker using spiral plate adsorbers, adsorption heat pump using novel heat exchanger as adsorbers, solar powered adsorption ice maker, solar powered hybrid system of water heater and adsorption refrigerator, waste heat driven air conditioning system for automobiles. Reasonable experimental results have been obtained, it was found that with a heat source temperature of 100°C, the refrigerator can obtain specific refrigeration power for 5.2 kg-ice/day per kg activated carbon in one adsorber, the heat pump can reach a specific cooling power for more than 150 W/kg-adsorbent with a COP close to 0.5, the adsorption solar ice maker yields 5–7 kg-ice per day per square meter solar collector, the hybrid solar water heater and ice maker is capable of heating 60 kg water up to about 90°C and meanwhile yields ice making about 5 kg per day with a 2 m^2 solar collector. The adsorption mechanisms of adsorption refrigeration pairs and also the thermo-physical properties have been also studied in SJTU, which are very helpful for adsorption refrigeration researches. This paper shows the various aspects researched in SJTU. © 2000 Elsevier Science Ltd. All rights reserved.

* Fax: +(86-21) 629 33250.
E-mail address: rzwang@mail.sjtu.edu.cn (R.Z. Wang).

PII: S1364-0321(00)00009-5

Nomenclature

A	constant of Clausius–Clapeyron equation
A_e	area of the solar collector (m^2)
a_b	thermal diffusion coefficient of bed (m^2/s)
a_f	thermal diffusion coefficient of fluid (m^2/s)
B	pore size of adsorbent (m)
C_{pa}	specific heat of adsorbent (kJ/kg·K)
C_{pf}	specific heat of thermal fluid (kJ/kg·k)
C_{pl}	specific heat of refrigerant liquid (kJ/kg·K)
C_{pm}	specific heat of metallic adsorber (kJ/kg.k)
C_{pwater}	specific heat of water (kJ/kg·K)
COP	refrigeration COP
COP_{cycle}	refrigeration cycle COP
$COP_{heating}$	refrigeration cycle COP driven by heating
COP_{solar}	solar power refrigeration COP
D	Adsorption parameter for an adsorption pair
f	fugacity (Pa)
$G(t)$	solar heat flux density (W/m^2)
h	wet perimeter of heat exchanger tube (m)
h_a	heat of adsorption (kJ/kg)
H_a	integrated heat of adsorption (kJ)
h_d	heat of desorption (kJ/kg)
H_d	integrated heat of desorption (kJ)
k	characteristic parameter of adsorption pair
K	adsorption parameter for D–A equation
L_e	latent heat of evaporation of refrigerant (kJ/kg)
M_a	mass of adsorbent (kg)
M_m	mass of metallic adsorber (kg)
M_{water}	mass of water in the tank (kg)
n	characteristic parameter of adsorption pair
P_c	condensing pressure (Pa)
P_e	evaporation pressure (Pa)
Q_c	heat to cool down the adsorber and adsorbent bed (kJ)
Q_{cc}	cooling consumed to cool down refrigerant from condensing temperature to evaporation temperature (kJ)
Q_g	Heat for isobaric generation process (kJ)
Q_h	Heat for isometric heating process (kJ)
Q_{hg}	Heat for desorption process (kJ)
Q_l	heat losses (kJ)
Q_{ref}	refrigeration effect (kJ)
Q_{reg}	heat regenerated (kJ)
Q_s	heat stored in the collector (kJ)

Q_T	total heat load (kJ)
Q_t	face heat losses (kJ)
Q_u	heat transferred to the water tank (kJ)
R	universal gas constant (J/mol·K)
R_{mf}	heat capacity ratio of adsorber material and thermal fluid to adsorbent
R_f	heat capacity ratio of adsorber material to adsorbent
R_m	heat capacity ratio of thermal fluid to adsorbent
SCP	specific cooling power (kW/kg-adsorbent)
SHP	specific heating power (kW/kg-adsorbent)
T	temperature (°C, K)
T_a	environmental temperature (°C)
T_{a1}	temperature to start adsorption (°C)
T_{a2}	adsorption temperature (°C)
T_b	adsorbent bed temperature (°C)
T_c	condensing temperature (°C)
T_e	evaporation temperature (°C)
T_f	thermal fluid temperature (°C)
T_{g1}	temperature to start desorption (°C)
T_{g2}	desorption temperature (°C)
T_p	average temperature of solar collector (°C)
T_s	saturated temperature (°C)
T_0	filled water temperature (°C)
U_b	bottom heat transfer coefficient (W/m²·K)
U_f	thermal fluid velocity (m/s)
U_t	face heat transfer coefficient (W/m²·K)
w	volume adsorption capacity (l/kg)
w_0	maximum volume adsorption capacity (l/kg)
x	adsorption capacity (kg-refrigerant/kg-adsorbent)
x_{dil}	adsorption capacity at desorbed state (kg/kg)
x_{conc}	adsorption capacity at adsorbed state (kg/kg)
x_0	adsorption capacity at a saturated pressure p_s corresponding to T_s (kg/kg)
Δ	half width of Guess normal distribution
α	absorptance, heat transfer coefficient (W/m²·°C)
β	affinity coefficient
ε	adsorption potential
ρ	density of refrigerant liquid (kg/m³)
τ	transmittance, time
η_{solar}	solar heating efficiency
Δx	adsorption capacity difference between adsorption phase and desorption phase $\Delta x = x_{conc} - x_{dil}$ (kg/kg)

1. Introduction

As a good opportunity to replace CFCs or HCFCs refrigeration, adsorption refrigeration research has got enough attentions during these years, specially its potential applications in waste heat recovery, solar energy utilization etc. The research extends not only in refrigeration itself, but also to Thermodynamics, Chemical Engineering, Material Science, New Energy, and specific technologies are involved. In recent years, various adsorption refrigeration cycles have been studied, however there are not enough verifications by prototype machines; not enough thermo-physical data measured such as specific heat, thermal conductivity, adsorption capacity; not enough consideration on adsorption mechanisms of adsorption refrigeration pairs; not much research on adsorption materials; not much considerations on the adsorption refrigeration applications.

Based upon the recent progress of adsorption refrigeration researches in Shanghai Jiao Tong University (SJTU), this paper concludes the various research aspects of adsorption refrigeration in SJTU, which includes adsorption mechanism, thermodynamic analyses of various adsorption refrigeration cycles, high performance prototypes of adsorption refrigerator and heat pump, application of adsorption systems in solar energy application and waste heat recovery.

2. Adsorption mechanism [1]

Dubinin–Astakhov equation (D–A equation) is commonly used to describe the adsorption of methanol or ammonia on activated carbon, water on zeolite, which is expressed as

$$x=x_0\exp\left(-k\left(\frac{\varepsilon}{\beta}\right)^2\right) \tag{1}$$

where x_0 is explained as limiting adsorption capacity, k is a constant determined by the structure of adsorbent, β is affinity coefficient which is determined by the adsorbent–adsorbate pair. ε is the adsorption potential energy. The reformed equation can be expressed as

$$w=w_0\exp\left[-D\left(T\ln\frac{p_s}{p}\right)^n\right] \tag{2}$$

$$x=x_0\exp\left[-K\left(\frac{T}{T_s}-1\right)^n\right] \tag{3}$$

where w and x represent the volume adsorption and mass adsorption respectively at temperature T and pressure p, in terms of the adsorbed liquid volume (l/kg) and the adsorbed liquid mass (kg/kg) per unit mass of adsorbent. In the above equations, p_s is the saturated vapor pressure corresponding to the adsorption temperature T, p is the adsorption pressure which is the saturated pressure corresponding to the saturated

refrigerant liquid temperature T_s, D, K and n are the adsorption parameters depending on the adsorption refrigeration pair, w_0, x_0 are the maximum adsorbed liquid volume and adsorbed liquid mass per unit mass of adsorbent respectively. The co-relations of the above two equations are

$$x_0 = \rho w_0 \tag{4}$$

$$K = DA^n. \tag{5}$$

The above D–A equations are widely adopted in adsorption refrigeration research, but the physical meaning of w_0 and x_0 are not clearly defined, as in the application of the two equations w_0 and x_0 are treated as constants. It can be seen from D–A equation that when the temperature of adsorbent T equals to the saturated temperature of refrigerant T_s, we get $x=x_0$. As is known in an adsorption capacity measurement, the different saturated temperature of refrigerant liquid T_s (which corresponds to different adsorption pressure) yields different value of x_0, thus the parameter of x_0 as the maximum adsorbed mass is not well defined. It might be estimated that the higher the adsorption pressure, the larger the adsorbed mass, its maximum will be the refrigerant mass occupying the all pore volumes of adsorbent.

A clear definition of adsorption capacity is

$$x = x(T,p) \tag{6}$$

which means the adsorbed mass in adsorbent is a function of adsorption pressure p and adsorbent temperature T. The above considerations have an assumption that the mini-pore sizes are nearly uniform in the adsorbent, a more generalized equation will be

$$x = x(T,p,B) \tag{7}$$

in which B corresponds to the mini-pore sizes of adsorbent. The pore size distribution can be assumed as

$$f(B) = \frac{1}{B_2 - B_1} \tag{8}$$

for uniform pore volumes (size between B_1 and B_2) or

$$f(B) = \frac{1}{\sqrt{2\pi\Delta}} \exp\left[-\frac{(B-B_0)^2}{2\Delta^2} \right] \tag{9}$$

for assumed Gauss normal distribution size with a half width of Δ.

For mathematical convenience, we may postulate a continuous distributions $f(B)$ for the adsorption concentration x_{0j}, and $x_{0j}=f(B_j)\delta B_j$. The sum is then replaced by the integral

$$\int_0^{\infty} f(B)\,\mathrm{d}B = 1. \tag{10}$$

Table 1
Adsorption parameters of three adsorption pairs correlated by Eq. (10)

Adsorption pair	x_0 (kg/kg)	B_0 ($\times 10^{-6}$ m^{-2})	Δ ($\times 10^{-6}$ m^{-2})
YKAC–methanol	0.294	1.033	0.289
SXAC–methanol	0.265	1.273	0.251
Zeolite–water	0.203	1.152	0.310

For a given size mini-pores characterized by B_j, adsorption equation can be treated as

$$x_j = x(T,p,B_j). \tag{11}$$

For an adsorption surface, the total adsorption capacity can be integrated with the characteristic adsorption of mini-pores multiplied by its distribution, thus we get:

$$x = \int_0^{\infty} x(T,p,B) f(B)\, \mathrm{d}B. \tag{12}$$

As limited in a very narrow range of pores, $\Delta B \to 0$, we may take, $x(T,p,B)=\text{const}=x_{B_i}$, $(B_1 \le B_i \le B_2)$ in this range. If fugacity f is used to replace pressure thus we get a simple form

$$x = x_i = x_{i0} \cdot \exp\left[-\left(\frac{RT\ln(f_0/f)}{E_i}\right)^{n_i}\right]. \tag{13}$$

From a mathematical view point, the general expression for the pore size with a Gauss distribution yields a Gauss-based general equation for the filling of pores

$$x = x_0 \exp(-B_0 y) \cdot \exp(y^2\Delta^2/2) \cdot [1-\mathrm{erf}(z)]/2. \tag{14}$$

This is the modified equation, where $z=(y-B_0/\Delta^2)\Delta/\sqrt{2}$, and erf($z$) is error function. The variable $y=(T/\beta)^2 \ln^2(f_0/f)$ already contains the adsorptive-dependent shifting factor β (affinity factor), and therefore simplifies the overall graphical representation, f represents fugacity of refrigerant which is used to modify the pressure terms in D–A equation. This equation contains three parameters: x_0, B_0 and Δ, which can be determined by adsorption experiments.

Typical values based upon the data treatment of adsorption capacity measurement are shown in Table 1 (activated carbon–methanol, zeolite–water) for heterogeneous distribution of adsorbent pore size and Table 2 (activated carbon fiber–methanol) for that of homogeneous distribution.

Table 2
Adsorption parameters of three ACF–methanol adsorption pairs correlated by Eq. (13)

Adsorption pair	x_0	E (kJ/mol)	n
JIAACF–methanol	0.342	6.703	1.346
SYACF–methanol	0.606	3.904	0.904
NTACF–methanol	0.602	7.674	1.272

3. Research on heat recovery adsorption refrigeration cycles [2]

Adsorption refrigeration is based upon the processes of heating–desorption–condensation and cooling–adsorption–evaporation, the cooling–adsorption process needs heat dissipation both of sensible heat and heat of adsorption. A two beds continuous adsorption refrigeration system with heat recovery is shown in Fig. 1. The schematic shows the operation when adsorber 1 is cooled and connected to the evaporator to get adsorption refrigeration in the evaporator, and adsorber 2 is heated and is connected to the condenser to get heating–desorption–condensation, the condensed refrigerant liquid flows into evaporator via a flow control valve. The operation phase can be changed, and the go-between will be a short time heat recovery process in which the two pumps drive the thermal fluid in the circuit between two adsorbers (the connection to the heater and cooler are blocked during this process). Heat recovery is important to increase the cycle COP, the possible heat recovery for a two adsorption bed system will be some part of sensible heat and heat of adsorption shown as Fig. 2. The COP for basic type adsorption refrigeration cycle (one bed or two beds without heat recovery) is

$$\mathrm{COP}_B=\frac{Q_{\mathrm{ref}}}{Q_{\mathrm{h}}+Q_{\mathrm{g}}}. \tag{15}$$

The COP for a two-bed heat recovery cycle can be expressed as

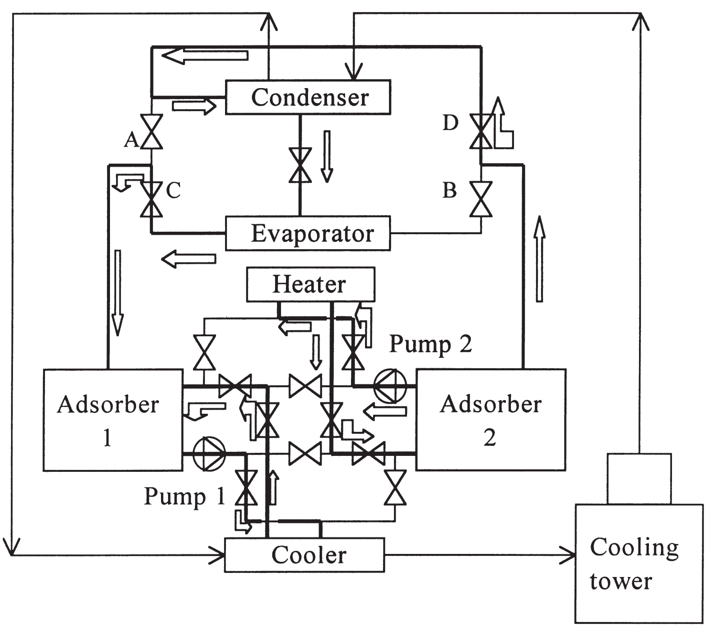


Fig. 1. Schematics of heat recovery two-beds adsorption refrigeration system.

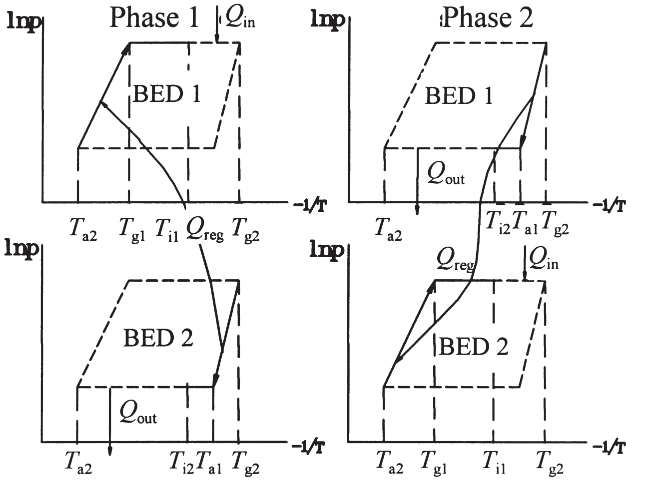


Fig. 2. Two-bed adsorption system with heat recovery. Operation phase 1: adsorbent bed 1 for heating and bed 2 for cooling, operation phase 2: adsorbent bed 1 for cooling and bed 2 for heating.

$$\mathrm{COP}=\frac{Q_{\mathrm{ref}}}{Q_{\mathrm{h}}+Q_{\mathrm{g}}-Q_{\mathrm{reg}}} \tag{16}$$

where Q_{reg} is the heat recovered. In the above equations, Q_h and Q_g are the heat for generation corresponding the two processes (isostersis and isobars). The refrigeration effect is approximately

$$Q_{\mathrm{ref}}=M_{\mathrm{a}}\cdot\Delta x\cdot L \tag{17}$$

if the sensible cooling of refrigerant liquid is neglected, which is the latent heat L multiplied by the cycle refrigerant mass $M_a\cdot\Delta x$.

As shown in Fig. 3, the cycle COP will be increased more than 25% by heat recovery process, but the COP for a single effect refrigeration system is still low, possibly in the range of 0.4–0.6. Multi-beds system will be good to recover more heat, thereby increase COP, however the real system will be very complicated.

For a real heat recovery adsorption system, the heat capacity of metallic adsorber and also the thermal fluid will have strong influence on system COP. If R_m is defined as the heat capacity ratio of adsorber material to adsorbent, and R_f that of thermal fluid to adsorbent, the total heat capacity ratio $R_{mf}=R_m+R_f$ will have strong influence on system COP. A typical example of the heat capacity ratio effect on system COP is shown in Fig. 4, as is seen the COP decreases significantly if the ratio R_{mf} increases. For example, when R_{mf}=10, the COP will decrease by 30–50% if compared with the ideal COP_0 (COP corresponding to R_{mf}=0). When R_{mf}=5, the COP decreases about 20–30%.

In real design of an adsorption system, good heat transfer should be considered, in order to shorten cycle time and increase specific cooling power (SCP), which may need to increase heat transfer area by finned tubes, etc. (Fig. 5). But the heat capacity

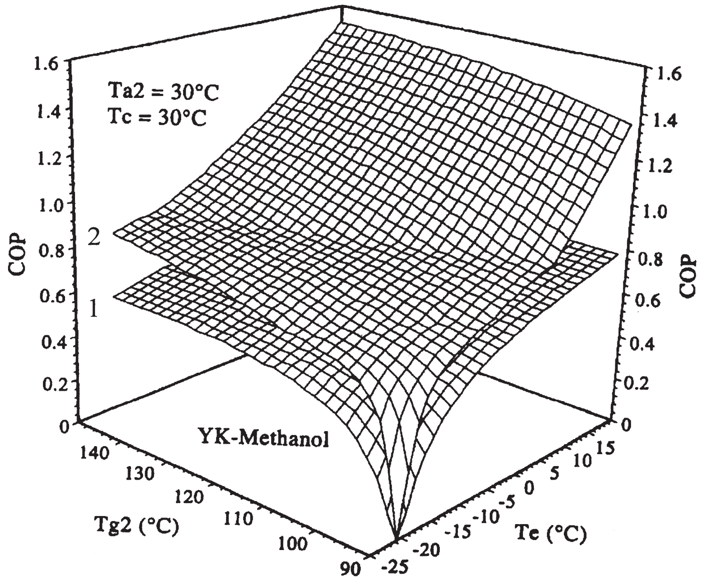


Fig. 3. COP with and without heat recovery. Evaporation temperature at −10°C, 1 — basic cycle, 2 — heat recovery cycle.

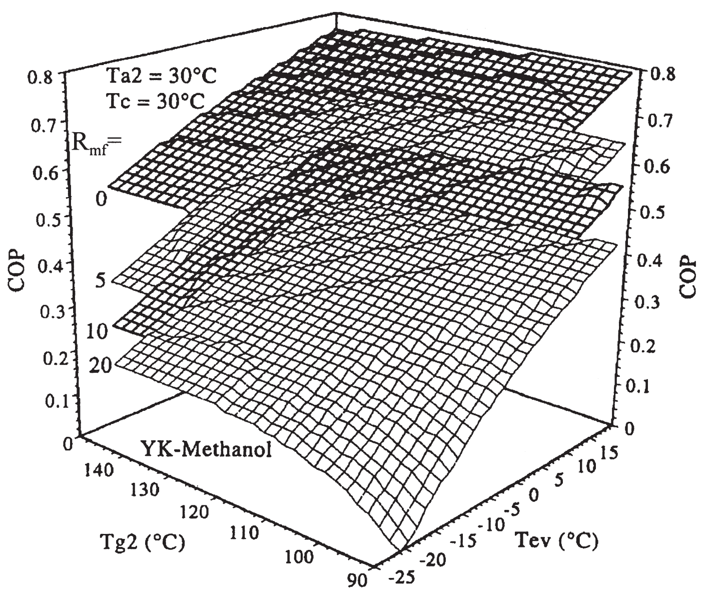


Fig. 4. Heat capacity ratio R_{mf} effect on COP of a heat recovery system.

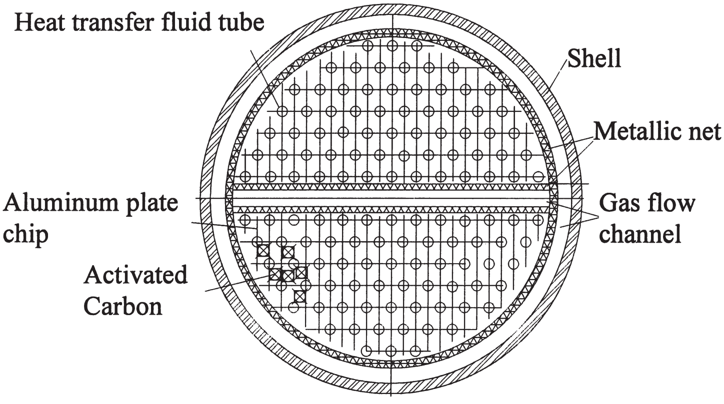


Fig. 5. A newly designed plate-finned tubes adsorber.

ratio should be controlled, the ideal value of R should be limited below 5, possibly below 3. Oil should be used as thermal fluid to decrease the heat capacity ratio R_f, also the flow volume of thermal fluid should be controlled.

Plate-fin heat exchanger and spiral plate heat exchanger have been applied as adsorbers because of very good heat transfer performance, the SCPs have been obtained as 150 W/kg-adsorbent for air-conditioning and 5.2 kg-ice/day/kg-adsorbent for ice-making, but the COPs are low due to the high values for both of R_f and R_m values. In the two systems, R_{mf} is high than 10, which causes the COP value relatively low [3].

An improvement has been made in activated carbon–methanol adsorption air-conditioning system, the newly designed plate-finned tubes adsorber is successful both for heat transfer and also the heat capacity control. The plate-finned tubes with a diameter of 9.5 mm are used for heat transfer between thermal fluid and adsorption bed, the aluminum plates are incorporated with the tubes to extend heat transfer surface. Adsorbent bed is packed by metallic net with the heat exchanger tubes, and a space to the shell is kept to have gas flow channels for enhancing mass transfer. Inside the adsorber, an extra mass flow channel is designed to separate the bed into two halves. The adsorber heat capacity ratio R_m=1.36, while the thermal fluid heat capacity ratio R_f=1.5 for water and R_f=0.53 for oil. The total heat capacity ratio is thereby controlled as R_{mf}=1.89 if oil is used as thermal fluid [3].

4. Heat and mass recovery adsorption refrigeration cycle

Mass recovery could be initiated followed by heat recovery (the ideal heat recovery state will be e-e′ for a two bed system shown in Fig. 6). As is clear, when adsorber 1 (as generator) is desorbed, it is at the generation temperature T_{g2} and condensing pressure P_c, which is to be cooled to serve as adsorber (temperature from T_{g2} to T_{a1}, pressure from P_c to P_e), while adsorber 2 (currently as adsorber) has adsorbed refrigerant, and is hoped to be heated to serve as generator (temperature

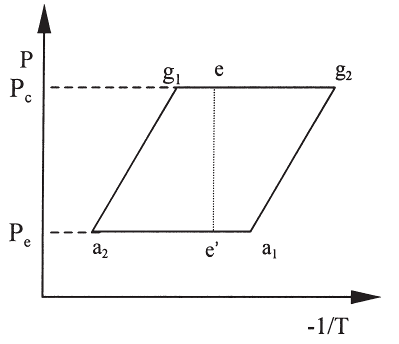


Fig. 6. Diagram of the intermittent and heat recovery cycle.

from T_{a2} to T_{g2}, pressure from P_e to P_c). A go-between connection between two adsorbers will speed up the pressure changes to reach equilibrium pressure $P_m=(P_e+P_c)/2$. This process will cause more desorption in the generator shown as Fig. 7.

The mass recovery cycle (a_2-a_3-g_1'-g_1-g_2-g_3-a_1'-a_2) extends the two bed basic cycle or two bed heat recovery cycle (a_2-g_1-g_2-a_1-a_2 shown as Fig. 6), and the cycle mass is increased from Δx to $\Delta x+\delta x$, which causes the refrigeration effect to increase. If the heat of adsorption and the heat of desorption is the same (at the same pressure), the cycle COP will increase as the increased refrigeration effect in a cycle. The typical comparison of COPs between basic type (two beds but without heat recovery) cycle and mass recovery cycle (two beds without heat recovery) are shown in Fig. 8.

The mass recovery process is usually before the heat recovery process, the combined mass and heat recovery procedures will contribute COP significantly. In the real system operation, heat recovery may have two kinds. One of which is sensible heat recovery, the other is sensible heat recovery followed by adsorption heat recovery. Fig. 9 shows the COPs of various operation procedures compared with basic type cycle and mass recovery cycle. It is seen that mass recovery followed by heat recovery (sensible and heat of adsorption) is of the best performance, and for acti-

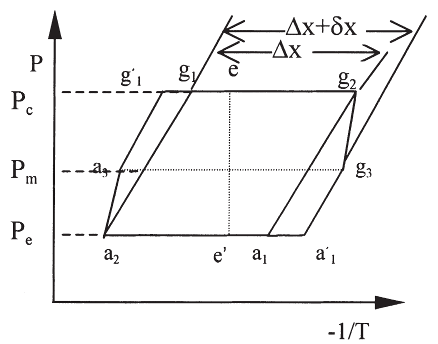


Fig. 7. Diagram of mass recovery cycle and heat and mass recovery cycle.

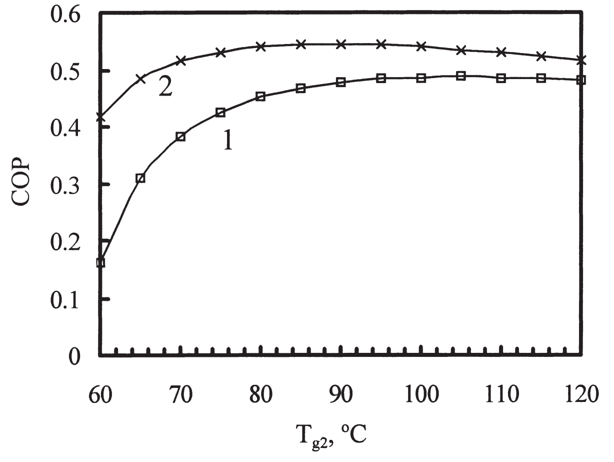


Fig. 8. Comparison of COPs for basic type cycle (1) and mass recovery cycle (2). T_e=5°C, T_c=T_a=30°C.

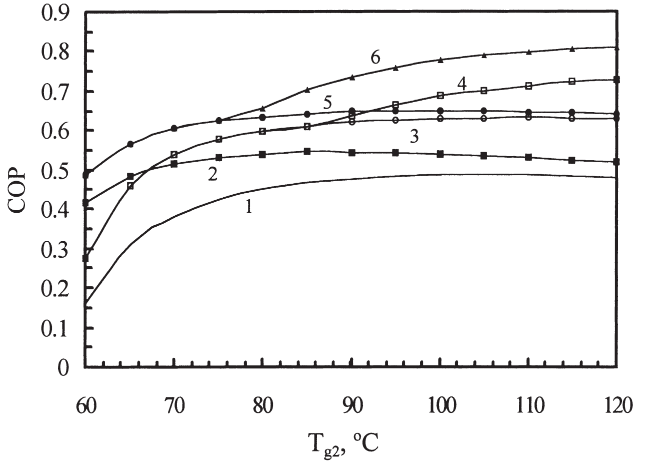


Fig. 9. Comparison of COPs for various operation procedures of heat and mass recovery cycle. T_e=5°C,T_c=T_a=30°C, R=0. 1, Basic type cycle; 2, mass recovery cycle; 3, sensible heat recovery; 4, sensible+adsorption heat recovery; 5, sensible heat and mass recovery; 6, Sensible+adsorption heat and mass recovery.

vated carbon–methanol air-conditioning system, COP over 0.6 can be achieved with a generation temperature of 80°C. If the generation temperature reaches 120°C, COP will be close to 0.8.

5. Thermal wave cycle [4]

Low COP is a main problem of the adsorption refrigeration. Many different cycles have been studied to improve the COP, with focus on improving the heat regenerative

ratio. One attractive cycle is the thermal wave cycle patented by Shelton [5]. The simulation of the cycle by Shelton showed that the heat regenerative ratio and COP for heat pump are as high as 70% and 1.87, respectively. Although many researchers have studied the cycle, up to now, there is no report of a successful prototype adopting thermal wave cycle. Oppositely, some experimental reports showed that the effect of the thermal wave cycle is very bad.

Thermal wave cycle utilizes a simple heat transfer fluid circulating loop for heating and cooling the two adsorbent beds, in which part of the adsorbent heat can be recovered from the bed being cooled to the bed being heated. Fig. 10 presents a typical thermal wave cycle system.

A heat transfer model [4] is established to investigate the thermal wave by analyzing the transient heat transfer between the fluid and the adsorption bed. Numerical method is adopted. The bed being heated is specially discussed.

Fluid:

$$\frac{\partial T_f}{\partial \tau}+U_f\frac{\partial T_f}{\partial x}=a_f\frac{\partial^2 T_f}{\partial x^2}-\frac{\alpha h}{\rho_f c_{pf} A_f}(T_f-T_b) \quad (18)$$

Adsorbent bed:

$$\frac{\partial T_b}{\partial \tau}=a_b\frac{\partial^2 T_b}{\partial x^2}+\frac{\alpha h}{\rho_b c_{pb} A_b}(T_f-T_b). \quad (19)$$

Here T is temperature, τ is time, A is the cross section area, h is the wet perimeter, U is the fluid velocity, a is thermal diffusion coefficient, α is the heat transfer coefficient. The subscripts f and b represent fluid and adsorbent respectively. Figs. 11 and 12 show the transient variation of the non-dimension temperatures of the fluid and the adsorbent along the bed. Shown as in Fig. 13, the temperature of the outlet fluid increases quickly, and the shape of the wave defined by Shelton becomes flat soon. Both of the two features are far from the ideal thermal wave, which charac-

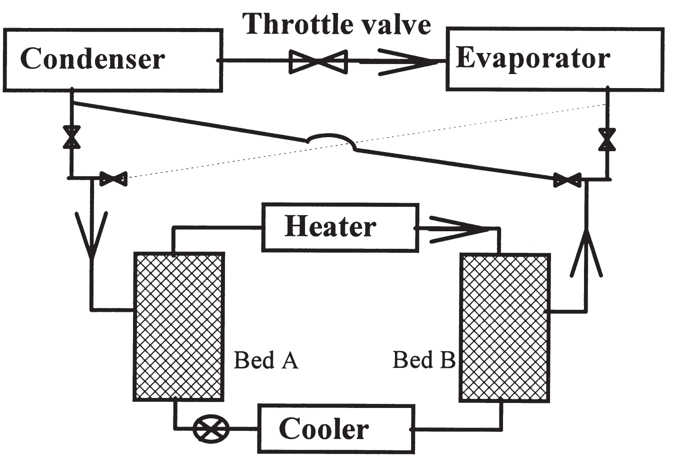


Fig. 10. The thermal wave cycle system.

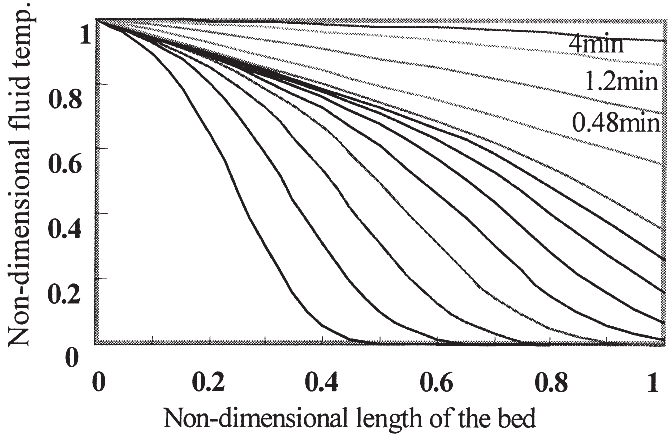


Fig. 11. The variation of the non-dimension temperature of the heating fluid along the bed during heating period α=100 W/m^2·°C, U_f=0.05 m/s.

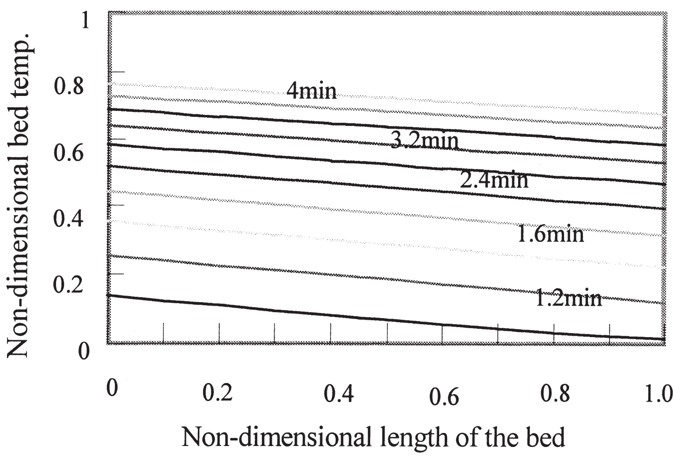


Fig. 12. The variation of the non-dimension temperature of the adsorbent along the bed during heating period.

terized by the steep and large temperature difference between the inlet and outlet fluid. As illustrated in Fig. 12, because the outlet fluid enters the cooler, the high temperature of the outlet fluid means that much heat is wasted in the cooler.

Fig. 13 shows the variation of the outlet fluid temperature under different conditions. The velocity of the heating fluid (U_f) and the equivalent heat transfer coefficient between the fluid and the adsorbent in the bed (α) are two main factors which influence the temperature of the outlet fluid. With low velocity of the fluid and high α, the temperature of the outlet fluid is able to increases slowly (such as U_f=0.05 m/s and α=2000 w/m^2°C). In addition, the velocity of the fluid plays a more important role, the temperature-increase curve with same α (such as α=1000, U_f=0.1

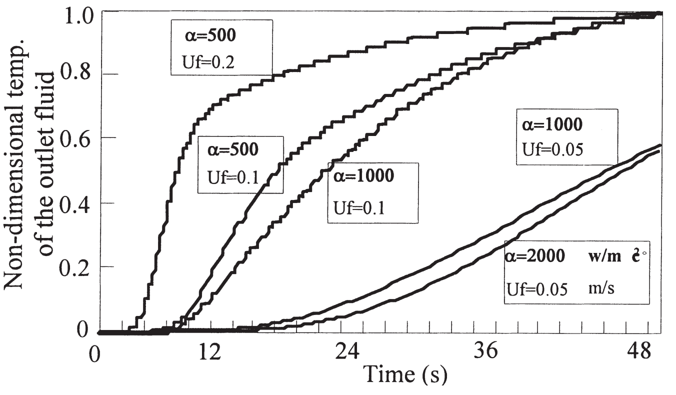


Fig. 13. Time dependent non-dimensional temperature of the outlet fluid.

and 0.05) differ greatly than the two curves with same U_f (U_f=0.1,α=500 and 1000). Because of the high velocity, the power transportation mainly flows in fluid direction, not in the perpendicular direction.

Ideal thermal wave cycle requires low U_f and high equivalent α. However, low velocity will result in very small heating capacity, which decreases the power density of the system. And because of the characteristic of the porous adsorbent, increasing of the equivalent α is greatly limited.

Fig. 14 shows the variation of the COP and SCP under different conditions. With the decreasing of the velocity, the COP increases, but the power density of the system decreases quickly. It is difficult to kill two birds with a stone.

It should be mentioned that the so-called thermal wave is a non-physical wave. Thermal wave is only a description of the fluid temperature, which mainly depends on the heat transfer condition. It does not have the features of many physical waves.

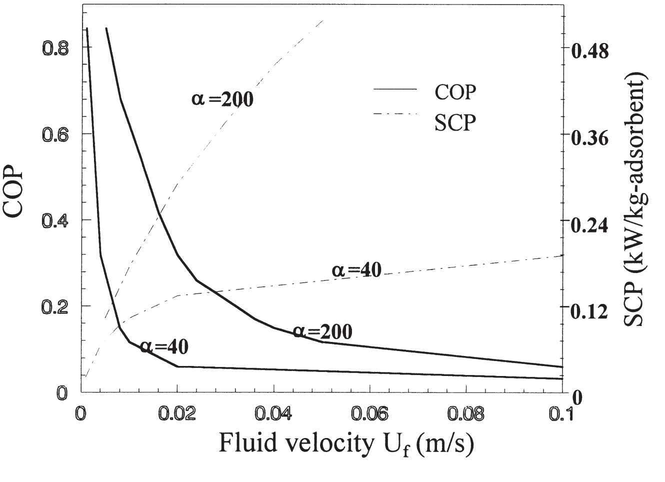


Fig. 14. The variation of the COP and SCP under different conditions

Some simulations of the thermal wave cycle just neglect this point. Many assumptions of physical wave have been applied to the thermal wave, and some promising results are obtained.

According to the above discussion, the following conclusions can be drawn: Two factors, the fluid velocity and the equivalent heat transfer coefficient, mainly influence the characteristic of the thermal wave. To achieve ideal thermal wave, the velocity of the fluid should be very low and the equivalent α should be high enough. However, low velocity of the heating fluid greatly decreases the power density of the system, and the increase of the equivalent α is greatly limited due to the characteristic of the porous adsorbent.

6. Convective thermal wave cycle

Based upon the concept of thermal wave cycle, the convective thermal wave cycle has been proposed by Critoph [6], in which the refrigerant is used as the heating/cooling medium, thus convective heat and mass transfer exists in the adsorption bed. As shown in Fig. 15, heat transfer to the bed from refrigerant convective vapor should be effective, it needs short time to get equilibrium state of adsorption during heating or cooling, and thereby the cycle time is usually short.

As shown in Fig. 15(a), refrigerant vapor is heated and cycled by a pump through adsorption bed, direct heat transfer between the heated refrigerant and adsorption bed is initiated, which causes the bed temperature goes up and thus desorption happens, the convective heat transfer coefficient is about 10^2~10^3W/m^2•K [7]. The refrigerant vapor pressure will increase up to condensing pressure, thus some part of the cycled convective vapor is condensed in the condenser and then is collected in the receiver, other part will be heated again through the heat exchanger and then cycled through the adsorption bed. When the heating–desorption process is finished, the system is switched to cooling–adsorption process, the pump will be reversed, and heating will be switched to cooling, the convective vapor is cooled in the heat exchanger and then cycled through the adsorption bed, cooling to the bed is initiated

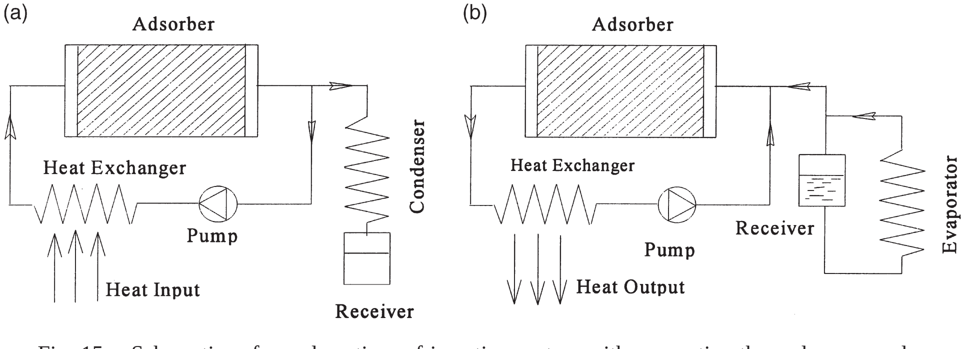


Fig. 15. Schematics of an adsorption refrigeration system with convective thermal wave cycle.

by the refrigerant vapor itself, adsorption process is then started, which causes evaporation of refrigerant liquid in the evaporator and refrigeration effect is obtained.

It is critical that a big temperature gradient should be obtained along the adsorption bed for both heating or cooling processes in the bed. The temperature gradient along the bed will be looked like a wave which moves along the cycle direction in the bed. The two phases of heating–desorption and cooling–adsorption is different procedures and thereby with different time. In real operation the two period could be assured as the same time for convince.

A simulation example has been taken for activated carbon fiber (ACF)–ammonia [7], in which ACF–ammonia has been used as the working pair, the adsorption bed of such example is shown in Fig. 16.

By assuming 1 kg ACF in the adsorber (250 mm in length), the condensing temperature of ammonia is 35°C, the evaporation temperature is −8°C, the heat driven temperature is 165°C,and the cooling temperature is 40°C, simulation to the thermal wave generation can be demonstrated in Figs. 17 and 18. In the simulation the vapor velocity in the bed inlet is assumed as 1 m/s, and the convective heat transfer between ammonia and the bed is 1050 $W/m^2 \cdot K$ at the condensing pressure of about 13.7 bar, and 433 $W/m^2 \cdot K$ at the evaporation pressure of about 2.7 bar. The simulated results for heating–desorption phase and cooling–adsorption phase are shown in Figs. 17 and 18 respectively, in which the running time is different. It is obvious that heating–desorption is more faster than that of cooling–adsorption. If the two phase time is kept the same, heat recovery will then be not so reasonable. Good control for the two phase operation is then very important. If we reduce the heating vapor velocity to 0.25 m/s, then the estimated heating time will be about 330 s which is almost equal to the cooling–adsorption time. The heat recovery rate is then about 0.4, and the refrigeration COP=0.78, heating COA=1.78. Table 3 shows the simulated results [7].

It is clear that convective thermal wave cycle is quite attractive, however the system is not so easy to build as it looks like. Critoph has tried such system, and has found that it is still possible to yield good operation performances [8].

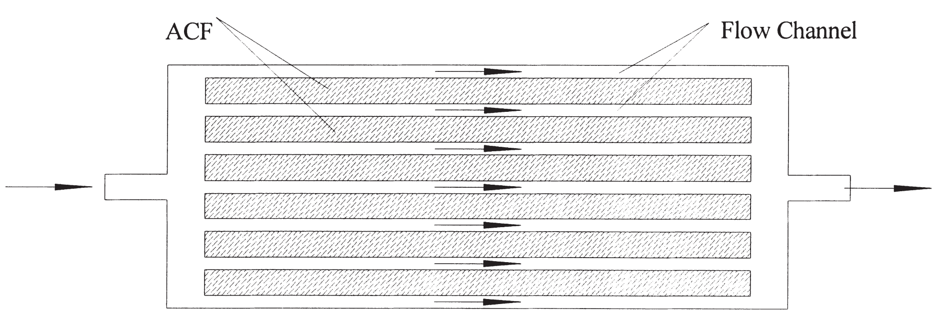


Fig. 16. ACF–ammonia adsorber for convective thermal wave cycle system.

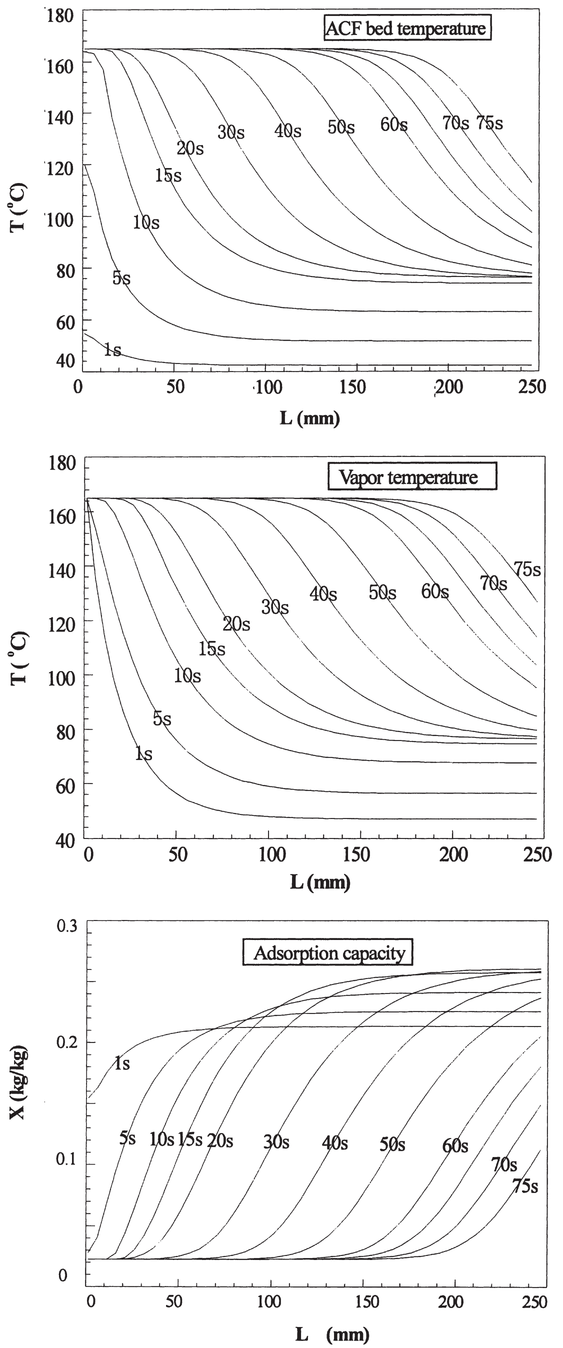


Fig. 17. ACF temperature, vapor temperature and adsorption capacity changes vs time during heating–desorption phase.

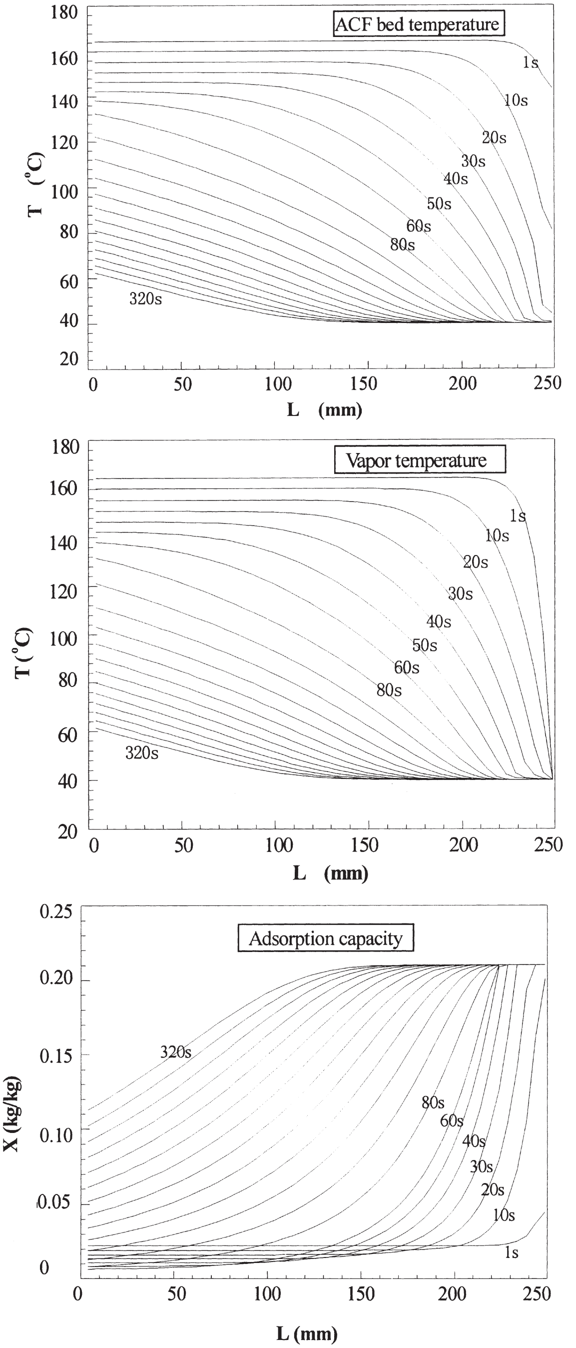


Fig. 18. ACF temperature, vapor temperature and adsorption capacity changes vs time during cooling–adsorption phase.

Table 3
A simulation example of convective thermal wave cycle

Heating gas temperature	165°C	Cooling gas temperature	40°C
Evaporation temperature	−8°C	Condensing temperature	35°C
Heat for generation	494.97 kJ	Heat rejected from adsorber cooling	470.93 kJ
Heat of condensing	271.73 kJ	Refrigeration effect	251.60 kJ
Heat recovered	192.904 kJ	Heat recovery ratio	40%
Heating/cooling time	330 s		
Refrigeration COP_C	0.7872	Heat pumping COP_H	1.78
Refrigeration SCP	760 W/kg	Heat pumping SPD_H	1616 W/kg

7. Multi-effect four-beds cascade cycle

The system configuration of a four-beds cascade adsorption refrigeration cycle is shown in Fig. 19. There are four adsorbers (A_1, A_2, B_1, B_2), one condenser (C), and one evaporator (E). Where A_1 and A_2 are in the high temperature stage, generation (temperature about 200°C) to this stage is initiated by heat input. The desorbed water vapor will go through the adsorber B_1 or B_2 at the low temperature stage to release heat for desorption. The adsorption pressure of the two stages are the same because only one evaporator is used in the system.

The working principle of the four-beds cascade adsorption refrigeration cycle can be described as:

1. Phase 1: A_1 of the high temperature stage is heated which serves as a desorber, while A_2 serves as an adsorber and is cooled by the heat rejection to the low temperature stage desorber B_1. In the low temperature stage, B_1 is a desorber while B_2 is an adsorber which is cooled by heat rejection to the heat sink. The desorbed water vapor from A_1 can go through B_1 for further heat recovery, though B_1 is normally heated by the cooling process of A_2. As shown in Fig. 20, C-1

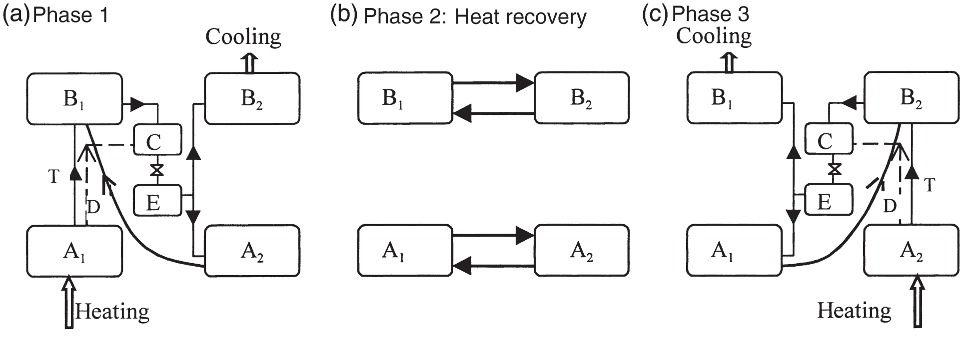


Fig. 19. The system configuration of four-beds cascade adsorption refrigeration cycle. T — triple effect arrangement, D — double effect arrangement.

process is the adsorption process of adsorber A_2, which is a heat release process, this heat (including sensible heat and heat of adsorption) is not rejected to outside, but to the desorber B_1 to generate the low temperature stage, which forms a double effect arrangement (the "D" arrangement in Fig. 19). If the desorbed water vapor from desorber A_1 (A_1 is now heated by outside) is introduced to desorber B_1 to increase the heat input (the "T" arrangement in Fig. 19), a triple effect arrangement is formed. Thus, cooling of adsorber A_2 is accomplished by the heat transfer to the desorber B_1, while cooling of adsorber B_2 is accomplished by the heat rejection to the outside environment via a cooler. Cooling effect is achieved by adsorption in A_2 and B_2. The ideal generation temperature T_7 of desorber B_1 will be equal to the adsorption temperature T_1 of the high temperature stage.

2. Phase 2: Heat recovery process in two stages: After the adsorption process in A_2 and B_2 on water (now as adsorbers) and the generation process of adsorbents in A_1 and B_1 (now as desorbers or generators), the heat recovery processes in the two stages are initiated by proper operation of valves. Adsorption can be started during this process if the bed pressure is lower than the evaporation pressure during the cooling process of the beds, which may provide an opportunities to recover some of the adsorption heat in addition to the sensible heat recovery. The heat recovery processes of the two stages stop at the respective heat recovery temperatures T_{reg2} and T_{reg1} , shown in Fig. 20. The heat recovery processes in the two stages will ensure good heat recovery, thus heating to generate the high temperature stage will be a d-3 process instead of a 1-2-d-3 process, and cooling the adsorber in the low temperature stage will be an f-5 process instead of 7-8-f-5 process.
3. Phase 3: A reversed phase of phase 1: After the heat recovery processes of the two stages, A_1 is changed into an adsorber and A_2 into a desorber in the high temperature stage, while B_1 acts as an adsorber and B_2 as a desorber.

The above process shows that the desorption process in phase 1 for desorber B_1 is furnished by the heat from desorber A_1 and adsorber A_2 in the high temperature stage. The coordination of adsorption and desorption of the two stages is very important to

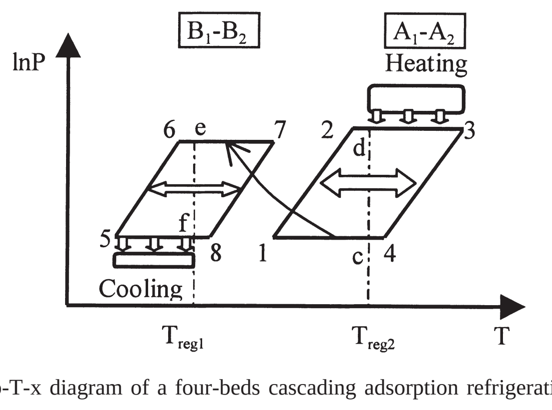


Fig. 20. p-T-x diagram of a four-beds cascading adsorption refrigeration cycle.

operate the system properly. By the way the desorption pressure in desorber A_1 should be higher than the desorption pressure of desorber B_1 in order to make the vapor desorbed from A_1 going through desorber B_1 properly. As has mentioned, water is the refrigerant in the cascade system, the desorbed vapor can go through the adsorbent bed in desorber B_1 to get a triple-effect installation.

Here a double effect is accomplished with sensible and adsorption heat recovery to generate low temperature stage in addition to the heat input to the high temperature stage, a triple effect is accomplished with the heat recovery of the desorbed vapor in the high temperature stage in addition to the heat used in a double effect arrangement to generate low temperature stage.

An ideal heat recovery process will make the intermediate temperature T_7 and T_1 the same. Here T_7 is the desorption temperature of low temperature stage adsorption cycle (5-6-7-8 in Fig. 20) and T_1 is the adsorption temperature of the high temperature stage adsorption cycle (1-2-3-4 in Fig. 20).

The maximum energy recovery from high temperature stage can be arranged by a triple effect system, in which the sensible heat of adsorbent bed, heat of adsorption and the latent heat of refrigerant vapor are fully used to drive the low temperature stage system. Assuming that the cascading triple effect adsorption cycle is composed by two independent continuous heat recovery adsorption refrigeration cycles, however the two stages are related each other by heat exchanging. The low temperature stage (the first stage) and the high temperature stage (the second stage) have COPs as COP_1 and COP_2 respectively, they can be expressed as:

$$\mathrm{COP}_1=\frac{Q_{\mathrm{ref1}}}{Q_{\mathrm{hg1}}-Q_{\mathrm{reg1}}} \tag{20}$$

$$\mathrm{COP}_2=\frac{Q_{\mathrm{ref2}}}{Q_{\mathrm{hg2}}-Q_{\mathrm{reg2}}}. \tag{21}$$

In reality, there are only heat input to stage 2 from outside, although the two stages contribute refrigeration effects Q_{ref1} and Q_{ref2} to furnish the total refrigeration Q_{ref}. Where Q_{hg} is the heat needed for heating generation which corresponds to the processes 1-2-3 or 5-6-7 of a single stage cycle in Fig. 20, Q_{reg} is the heat recovered from the heat recovery process.

The COP of a double effect cascade adsorption cycle can be defined as

$$\mathrm{COP}=\frac{Q_{\mathrm{ref}}}{Q_{\mathrm{hg2}}-Q_{\mathrm{reg2}}}=\frac{Q_{\mathrm{ref1}}+Q_{\mathrm{ref2}}}{Q_{\mathrm{hg2}}-Q_{\mathrm{reg2}}}. \tag{22}$$

If Eq. (21) is applied to Eq. (22), then

$$\mathrm{COP}=\mathrm{COP}_2+\mathrm{COP}_1\cdot\frac{Q_{\mathrm{hg1}}-Q_{\mathrm{reg1}}}{Q_{\mathrm{hg2}}-Q_{\mathrm{reg2}}}. \tag{23}$$

According to the first law of thermodynamics, to the high temperature stage we have

$$Q_{\mathrm{hg2}}+Q_{\mathrm{ref2}}=Q_{3\text{-}4\text{-}1}+Q_2. \tag{24}$$

In which Q_2 is the heat released from the desorbed vapor to low temperature stage,

$Q_{3\text{-}4\text{-}1}$ is the sensible heat of cooling process together with the heat of adsorption of the second stage. In ideal case, the heat released from high temperature stage is used thoroughly to generate the low temperature stage, which gives

$$Q_{hg1}-Q_{reg1}=(Q_{3\text{-}4\text{-}1}-Q_{reg2})+Q_2. \tag{25}$$

If Eqs. (24) and (25) are used, then Eq. (23) can be expressed as

$$\mathrm{COP}=\mathrm{COP}_2+\mathrm{COP}_1\cdot\frac{Q_{hg2}-Q_{reg2}+Q_{ref2}}{Q_{hg2}-Q_{reg2}} \tag{26}$$

$$\mathrm{COP}=\mathrm{COP}_2+\mathrm{COP}_1\cdot(1+\mathrm{COP}_2)=\mathrm{COP}_1+\mathrm{COP}_2+\mathrm{COP}_1\cdot\mathrm{COP}_2. \tag{27}$$

The above equation shows clearly the relation between the cascading cycle COP and two independent stage cycle COP_1 and COP_2. A typical example is that if both stages have COP=0.6, then the triple effect cascading COP=1.56.

This concept could be used for multi-effect adsorption systems, and also adsorption–absorption cascading systems [9,10].

8. Hybrid heating and cooling cycle

The schematic design of a hybrid solar powered water heater and refrigerator is shown in Fig. 21. The system consists of a solar collector, water tank, adsorber/generator, condenser, evaporator, receiver and ice box and so on.

The working principle is just a combination of a solar water heater and adsorption refrigeration. Heating of the water tank is started in the morning through vacuum tube type solar collector. With the increasing of the water temperature, the temperature in the adsorbent bed rises. In an ideal process, the adsorbent temperature could be very close to the water temperature in the tank. When the temperature in the adsorbent rises up to a temperature (T_{g1}) which causes the vapor pressure of the desorbed

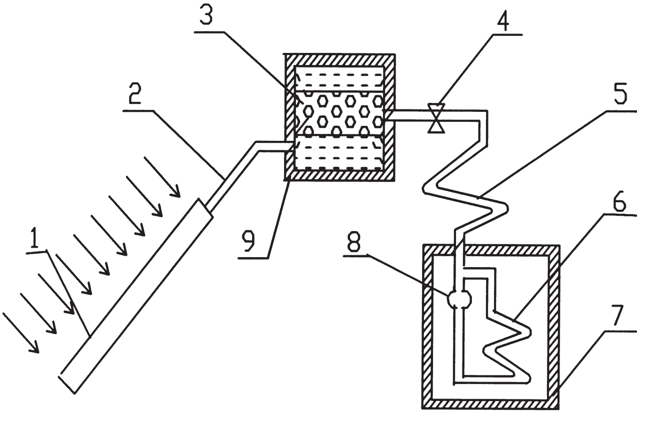


Fig. 21. Schematic of the solar water heater and refrigerator. 1, Solar collector; 2, water pipe; 3, adsorber; 4, valve; 5, condensor; 6, evaporator; 7, refrigerator (with cold storage); 8, receiver; 9, hot water container.

refrigerant up to the condensing pressure (P_c), desorption at constant pressure is initiated, the desorbed vapor is condensed in the condenser and collected in the receiver. This liquid flows to the evaporator via an flow rate regulating valve. The temperature of the water and the adsorbent bed continues rising due to solar heating, a maximum temperature (T_{g2}) for 80–100°C could be achieved at the end of the process. The high temperature water is used in the evening for the family, also the hot water in the tank could be drained out and moved into another tank at home, thus hot water can be used very flexibly.

With the refilling of the water tank with cold water, the temperature of the adsorbent bed is reduced rapidly ($T_{g2} \rightarrow T_{a1}$), and the pressure in the adsorber drops to a value below evaporation pressure (P_e). Evaporation could happen if the connecting valve is open, and ice will be made in the refrigeration box. The cooling of the adsorber and the rejection of adsorption heat may cause the temperature of cold water in the tank to rise several degrees ($T_0 \rightarrow T_{a2}$), however this energy is not wasted. Several degrees high than cold water temperature (T_0) will not influence much the adsorption refrigeration, this might be even better than normal cooling to the adsorption bed by natural convection. Refrigeration will continue for the whole night until the next morning. The thermodynamic cycle for adsorption refrigeration can be demonstrated in a P-T-X diagram shown as Fig. 22.

The features of the hybrid system include (1) water heating and refrigeration with one solar collector, which is suitable for household applications; (2) adsorber/generator is separated from collector, thus high efficiency vacuum collector can be used for water heating, thereby heating the adsorber at same time. The high efficiency heating does not mean a bad cooling of the adsorber through the night, as by draining the hot water from the tank, cold water is refilled to the tank, thus the adsober is cooled and refrigeration will take place; (3) energy efficiency is high for the use of the total solar energy collected; and (4) there is no danger of methanol disintegration as the maximum temperature of adsorbent bed cannot exceed 100°C, due to the water tank.

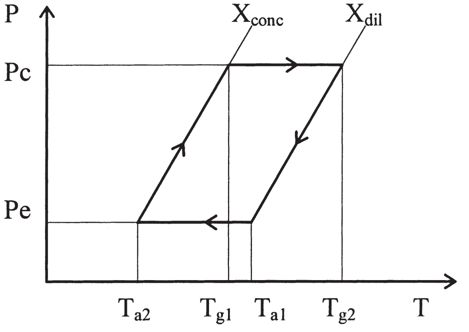


Fig. 22. Adsorption refrigeration cycle in hybrid solar water heater/ice maker.

8.1. Energy analysis of solar heating

Solar heating absorbed by the collector will be used in three ways: (1) Q_u, energy to heat the water tank and adsorbent bed, (2) Q_s, energy storage in the collector; (3) Q_l, energy lost due to various losses. The energy conservation equation is

$$A_e G(\tau\alpha) = Q_u + Q_1 + Q_s \quad (28)$$

where G is the solar flux density to the adsorber, τ is the transmittance of solar radiation through the cover of the collector, α is the absorptance of the collector, A_e is the area of the collector.

For a plate type or evacuated tube type solar collector, the heat quantity Q_u is used to heat the water and adsorber in the water tank, which is mainly determined by the efficiency of collector; The heat quantity Q_s is dependent on the solar collector material; Q_l is the heat losses composed of the face loss Q_t, the bottom loss Q_b, and the four sides loss Q_e. Usually Q_e is relatively smaller than Q_t and Q_b, in which Q_t and Q_b can be calculated by

$$Q_t = \int U_t A_e (T_p - T_a)\, dt \quad (29)$$

$$Q_b = \int U_b A_e (T_p - T_a)\, dt. \quad (30)$$

Here T_p is the average temperature of solar collector, T_a is the environmental temperature, U_t is the heat loss coefficient of the collector face, U_b is the heat loss coefficient of the collector bottom. Of the heat losses, Q_b is usually less than 10%.

8.2. Energy analysis of the adsorber in the water tank

The useful heat from the collector Q_u, will contribute both to the heating of the water in the tank and to the heating of the adsorber which will cause the desorption of refrigerant from the adsorbent bed. The energy equation can be written as

$$Q_u = \int_{T_{a2}}^{T_{g2}} M_{water} C_{water}\, dT + \int_{T_{a2}}^{T_{g2}} (M_m C_{pm} + M_a C_{pa})\, dT + \int_{T_{a2}}^{T_{g1}} x_{conc} M_a C_{pl}\, dT \quad (31)$$
$$+ \int_{T_{g1}}^{T_{g2}} h_d M_a\, dx + \int_{T_{g1}}^{T_{g2}} x(T,p_c) M_a C_{pl}\, dT.$$

In which the first term represents the heat added to the water bath in the tank, the second term is the sensible heat of the metallic tank and adsorbent mass. Item 3 is the sensible heat of refrigerant liquid in the adsorbent before desorption, item 4 is the heat of desorption, item 5 is the sensible heat of refrigerant remained in adsorbent

bed. In Eq. (31), M_{water}=mass of water, C_{water}=specific heat of water, M_m=mass of adsorber, C_{pm}=specific heat of adsorber, M_a=mass of adsorbent, C_{pa}=specific heat of adsorbent, C_{pl}=specific heat of refrigerant in the adsorbed state. Heat of desorption can be described by

$$H_d=\int_{T_{g1}}^{T_{g2}} h_d M_a \,dx=\int_{T_{g1}}^{T_{g2}} h_d M_a \frac{dx}{dT}\,dT \tag{32}$$

here h_d is the heat of adsorption, which is a function of x.

In the research, activated carbon–methanol is used as the working pair. The adsorption equation of activated carbon–methanol can be described by equation [11]:

$$x=x_0 \exp\left[-k\left(\frac{T}{T_s}-1\right)^n\right] \tag{33}$$

where x is the adsorption capacity, k and n are the characteristic parameters of adsorption refrigeration pair, x_0 is the adsorption capacity at $T=T_s$ and $P=P_s$ (where T_s is the saturation temperature at pressure P_s), T is the adsorption temperature. Typical parameter values for the activated carbon–methanol pair are: x_0=0.284, k=10.21, n=1.39, T_s=288.3 K, where Shanghai “YK” (coconut shell type activated carbon) is used. h_d can be calculated from Clausius–Clapeyron equation, where $T_s=T_c$ (condensing temperature):

$$h_d=RA\frac{T}{T_c} \tag{34}$$

here R is the gas constant and A is the constant of Clausius–Clapeyron equation.

8.3. Energy balance between filled water and adsorber

In the evening, the hot water in the tank is drained into another storage tank or is used directly. Cold water is then filled into the tank to cool the adsorber. The sensible heat of adsorber and the heat of adsorption will cause the filled water rises its temperature for several degrees, thus this energy will not be lost. The adsorption temperature T_{a2} is determined by the energy balance between the filled cold water and the adsorber to be cooled.

The sensible heat for cooling the adsorber bed from T_{g2} to T_{a2} is

$$Q_c=\int_{T_{a2}}^{T_{g2}} (M_m C_{pm}+M_a C_{pa})\,dT+\int_{T_{a1}}^{T_{g2}} x_{dil} M_a C_{pl}\,dT+\int_{T_{a2}}^{T_{a1}} h_a M_a\,dx+\int_{T_{a2}}^{T_{a1}} x M_a C_{pl}\,dT \tag{35}$$

where item 1 is the sensible heat of adsorber mass and adsorbent, item 2 is the sensible heat of refrigerant in adsorbent bed, item 3 is the heat of adsorption, which can be calculated as

$$H_a = \int_{T_{a2}}^{T_{a1}} h_a M_a \, dx = \int_{T_{a2}}^{T_{a1}} h_a M_a \frac{dx}{dT} \, dT \quad (36)$$

item 4 is the sensible heat of adsorbent during adsorption process. The sensible heat for cooling is transferred to the filled cold water in the tank. This may cause the temperature increase for several degrees of the water in the tank.

If water has a temperature T_0 before adsorption, then the water temperature after adsorption is

$$T_{a2} = T_0 + \frac{Q_c}{M_{water} \times C_{pwater}} \quad (37)$$

which is also the adsorption temperature for the refrigerator.

8.4. Refrigeration capacity

The desorbed refrigerant is condensed in the condenser and flows into the evaporator. When the adsorbent bed pressure is lower than evaporation pressure, the refrigerant liquid in the evaporator will evaporate which causes the refrigeration effect. The refrigeration quantity is

$$Q_{ref} = \Delta x M_a L_e \quad (38)$$

$$\Delta x = x_{conc} - x_{dil} \quad (39)$$

where L_e is the latent heat of vaporization, x_{conc} is the adsorbent capacity before desorption and x_{dil} is the adsorption capacity after desorption.

Some of the cooling quantity will be consumed to cool the refrigerant liquid from condensing temperature T_c to evaporation temperature T_e

$$Q_{cc} = M_a \Delta x C_{pl} (T_c - T_e). \quad (40)$$

8.5. Refrigeration COP_{cycle} and system COP_{solar}

Refrigeration Cycle COP can be written as

$$COP_{cycle} = \frac{Q_{ref} - Q_{cc}}{Q_g} \quad (41)$$

where Q_g is the heat for the regeneration of the adsorption bed, which is shown as

$$Q_g = Q_u - Q_{water} = \int_{T_{a2}}^{T_{g2}} (M_m C_{pm} + M_a C_{pa}) \, dT + \int_{T_{a2}}^{T_{g1}} x_{conc} M_a C_{pl} \, dT + \int_{T_{g1}}^{T_{g2}} h_d M_a \, dx$$

$$+\int_{T_{g1}}^{T_{g2}} xM_a C_{pl}\,dT \tag{42}$$

$Q_{water}=\int_{T_{a2}}^{T_{g2}} M_{water}C_{water}\,dT$ is the sensible heat to heat the water in the tank, here the sensible heat to heat the tank is neglected.

In a normal solar powered ice-maker, the collector is in the same unit of adsorber, Q_{water} is zero, Q_u is the whole contribution of heating to the adsorber. In this case the energy Q_c must be taken away in the evening and the whole night to furnish the refrigeration effect. Cooling by normal convection is difficult to release Q_c.

The hybrid system has two useful output, one is refrigeration, its solar efficiency is

$$\mathrm{COP}_{solar}=\frac{Q_{ref}-Q_{cc}}{\int G(t)\,dt} \tag{43}$$

another is heating the water in the tank, its solar efficiency is

$$\eta_{solar}=\frac{Q_{water}}{\int G(t)\,dt} \tag{44}$$

where $G(t)$ is the solar flux density, $\int G(t)\,dt$ is the total solar energy during the whole day.

A prototype hybrid system for water heating and ice-making has been developed, the adsorber is consisted of 28 $\phi 50\times 1\times 750$ mm stainless steel tubes, in which 22 kg activated carbon was filled, the adsorber mass is about 25 kg. The water tank is filled with 120–150 kg water. A 1500 W electric heater is used to simulate a 3 m^2 evacuated heat pipe type solar collector.

A typical experiment is demonstrated, the initial water temperature in the water tank is 18°C, and the initial adsorbent temperature is 20°C. After 6 h heating, the 150 kg water bath temperature reaches 81°C, and the adsorbent temperature reaches 72°C. The desorption process starts, in a 4 h desorption process heating to the water bath continues. The stop point of heating is 98°C for water bath, the corresponding desorption temperature is 89°C. The desorbed methanol is 4.1 liters, about 3.3 kg. About 54 MJ heat is added in the 10 h heating–desorption process.

The hot water was taken away in the evening at 20:00, then the city water with a temperature of 10°C was filled into the tank, the adsorbent bed temperature was thereby reduced to 27.4°C. Meanwhile about 15 kg water with a temperature of 15°C was filled into the ice box. Adsorption refrigeration was then initiated, which lasted until the next morning at 8:00. What measured were: the water bath temperature

Table 4
The experimental results of the hybrid system [11]

Experimental date	Energy accepted (MJ)	Hot water output		Ice output		COP_{system}	COP_{cycle}	η_{system}
		°C	kg	°C	kg			
9–10 December 1998	54	98	150	−2.5	10.5	0.067	0.386	0.906
10–11 March 1999	49	91.3	112	−1.8	10	0.064	0.431	0.758

raised up to 17.4°C, the adsorbent temperature decreased to 22°C. It was found that 10.5 kg ice with a temperature of −2.5°C had been made.

Here the definition of COP and η correspond to Eqs. (43) and (44) are

$$COP_{heating}=\frac{Q_{ref}-Q_{cc}}{Q_T} \tag{45}$$

$$\eta_{heating}=\frac{Q_{water}}{Q_T} \tag{46}$$

where Q_T is the total heat added from the heater to the water bath. It was evaluated that the adsorption refrigeration COP driven by heating is $COP_{heating}$=0.067, and the heating efficiency is $\eta_{heating}$=0.906. The adsorption refrigeration cycle COP has been calculated as COP_{cycle}=0.386.

Table 4 shows the two experimental results of hot water and ice output in two typical seasons: winter and spring. The water bath is relatively big, in which 150 kg water and 112 kg water were filled for testing. In order to get the designed value in which hot water output is about 60 kg with a 2 m^2 solar collector heat input, calculations based upon the above tests shown in Table 4 were done, Table 5 shows the results. Here 60 kg water is assumed in the water bath, the energy accepted is about 22–24 MJ per day, which is a simulation to a 2 m^2 solar collector. The calcu-

Table 5
Calculated performance of the hybrid system based upon experimental results

Experimental date	Energy accepted (MJ)	Hot water output		Ice output		COP_{system}	COP_{cycle}	η_{system}
		°C	kg	°C	kg			
9–10 December 1998	24.6	98	60	−2.5	10.5	0.143	0.386	0.795
10–11 March 1999	22	91.3	60	−1.8	10	0.144	0.431	0.797

lated results show that a 2 m^2 solar collector is capable of heating 60 kg water to about 90°C and producing ice for about 10 kg.

Attention should be made that the demonstration prototype system of water heating is in an open tank, in which the cover of the tank is not sealed, which caused about several percent heat dissipation by evaporation of water. The value of η_{system} is thus smaller than the ideal system, so is the COP_{system}.

A typical operation for the hybrid solar powered water heater and ice-maker is shown in a p-T-x diagram as Fig. 23, the recorded parameters of the operation show that the operation is in good agreement with theoretical expectation in Fig. 22, the temperature increase of water in the water box shows that the sensible heat of the adsorber and the heat of adsorption is recovered effectively, this heat has been thereby stored in the water.

Recent experimental work has proved that an one day operation will not only contribute hot water, but also yield refrigeration for a 120 liter cold box for more than 50 h with a temperature less than 5°C.

9. Performances of an adsorption refrigerator and a heat pump

9.1. Adsorption refrigerator

A prototype continuous heat regenerative adsorption refrigerator using activated carbon–methanol has been developed [12]. In the adsorption system, two adsorbers are independently operated for heating or cooling along with the intermediate heat recovery process. Fig. 24 shows the whole unit and measuring sensors. The system has two adsorbers, one condenser and one evaporator, a receiver is installed for the observation of refrigerant flow in the system. There are 6 kg activated carbon in each adsorber.

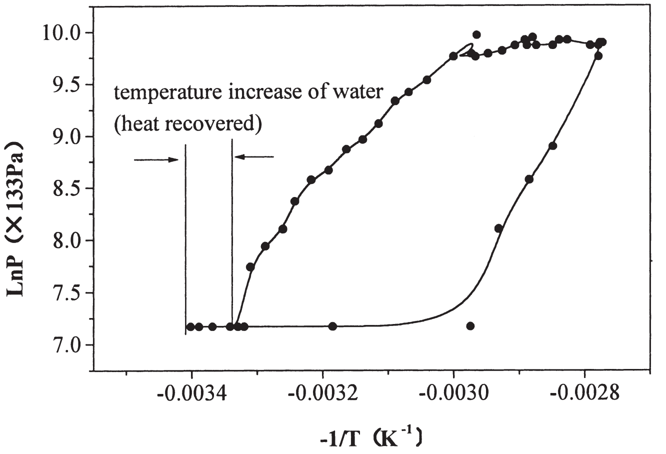


Fig. 23. A typical operation of the hybrid solar water heater and ice maker in p-T-x diagram

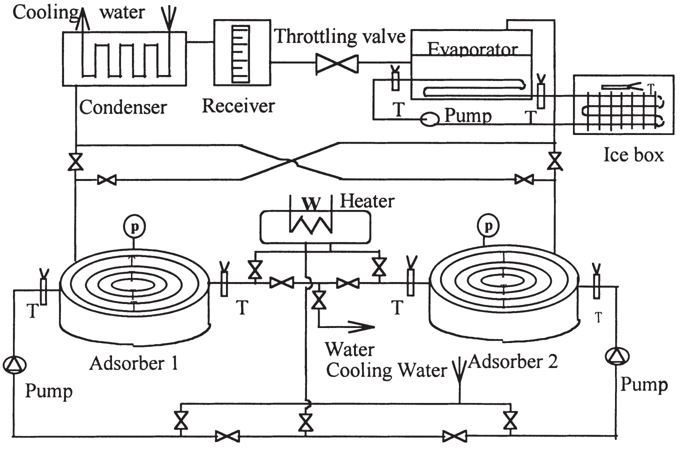


Fig. 24. Schematic of a prototype heat regenerative adsorption refrigerator.

The connections of the two adsorbers to the condenser and evaporator are by four vacuum valves, which keep one adsorber when regenerated being connected to the condenser and the other adsorber when cooled for adsorption connected to the evaporator. Heating to an adsorber is controlled by a computer, the measured data of every sensor are shown on the display of computer.

The above system has been applied for ice-making, which can show its application potentials for waste heat driven ice-making.

The ice-making test results with indirect evaporator [12] and direct evaporator [13] are shown in Table 6, the direct evaporation shows a big improvement in ice

Table 6
Experimental performance for ice-making with direct evaporation

Experimental working condition	Indirect refrigeration		Direct evaporation			
	1	2	3	4	5	6
Cycle time (min)	40	40	60	80	100	100
Adsorption temperature T_a (°C)	25	30	33.5	33	33.6	32.5
Desorption temperature T_d (°C)	100	101.5	91	92	92.3	96.7
Condensing temperature T_c (°C)	22	30	31.5	32	32.1	31.6
Evaporation temperature T_e (°C)	−15	−13.5	−15.5	−15.3	−15.5	−15
Ice made per day (kg)	14.6	13.25	24	26	30	31.5
Specific cooling power SCP (kg-ice/adsorber kg-carbon per day)	2.44	2.20	4.0	4.34	5.0	5.26

making. It can be observed though with the low desorption temperature or high condensing and adsorption temperatures. The test results proves that it is possible to achieve a SCP for ice-making of more than 5.2 kg-ice per day per adsorber kg activated carbon. By the way the optimized cycle time is quite different if compared with the indirect evaporation, which is perhaps caused by different heat transfer area and also the difference of heat losses in the evaporator. In this test, the optimized cycle time is 100 min for direct evaporation, and 40 min for indirect evaporation. The COP for ice making test is about 0.13 for typical operation condition 6 in Table 6.

It is shown that good SCP values have been obtained, but the system COP is still very low. This is perhaps mainly caused by the big mass of adsorber. In the design, the adsorber has a weight of 80 kg (mainly the two upper flanges) and the adsorbent only 6 kg per adsorber, large amount of sensible heat is wasted to heat the stainless steel heat exchanger and thermal fluid. The real machine does not need the flanges like the prototype system, which may show better performance results. By the way the water thermal fluid is used which has also a big heat capacity.

The research progresses on heat regenerative adsorption refrigerators show that

1. Spiral plate heat exchanger is suitable for adsorber however the heat capacity of the adsorber body has a strong influence on the COP. In a real machine, the two flanges are not necessary, which will reduce the mass of adsorber obviously.
2. A good design of an adsorption refrigerator should consider the match of condenser, evaporator and adsorber/generator. In the operation of a system, means should be provided to get the real operation close to ideal processes.
3. Our system has been improved step by step, which is now capable of specific cooling power of 5.2 kg-ice/adsorber kg-adsorbent per day with a generation temperature less than 100°C.

9.2. Adsorption heat pump

An adsorption heat pump for air conditioning using plate fin heat exchangers as adsorbers has been developed in SJTU [14], in which activated carbon–methanol has been used as adsorption pair. The system has two adsorbers, each of which has 26 kg carbon embedded, the plate fin type adsorber makes the heating and cooling for adsorbers quite quickly. The system can be operated in a cycle time as short as 20 min. As shown in Fig. 25, the system is very close to the adsorption system for ice-making, though the cooling is output to a fan-coil (actually two fan-coils each has 5 kW cooling power were used for the experiment) and a cooler is used to cool the thermal fluid of adsorber by cooling water from the cooling water tower.

A novel type adsorber has been designed, which is a plate finned shell and tube heat exchanger, shown as Fig. 5, the designed heat capacity ratio between adsorber mass plus thermal fluid and adsorbent bed is 2.86 when water is used as thermal fluid, however good heat transfer is still possible to obtain. Two newly adsorbers were installed in the adsorption heat pump system, each of them were embeded with 26 kg activated carbon.

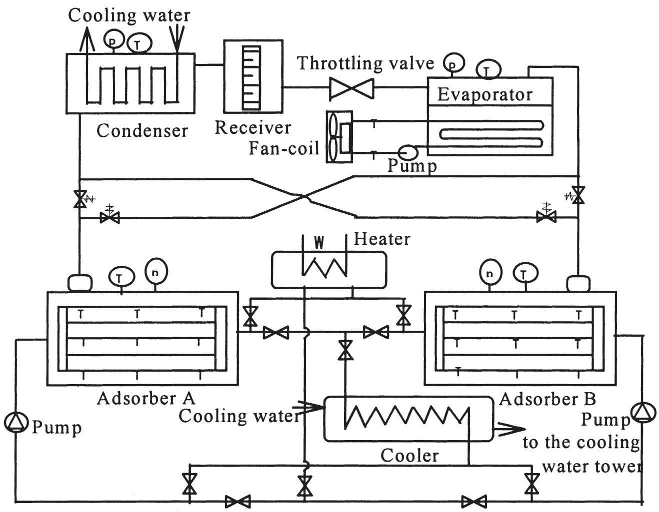


Fig. 25. Schematic drawing of the whole adsorption heat pum system.

Some tests were performed to the improved adsorption heat pump with novel configured adsorbers. After various experiments, it was found that the best cycle time for this adsorption heat pump is between 40–50 min with a heat recovery time for about 2 min. Several typical experiments were done with the following environmental parameters: room temperature=24°C, cooling water temperature=23.5°C and flow rate of chilled water=1.157 m^3/h, thus the performances of the system can be evaluated.

The measuring schemes are: (1) heat source temperature (T_h): 100°C, evaporation temperature (T_e): 10°C, cycle time (t): 50 min; (2) T_h =100°C, T_e=10°C, t=40 min; (3) T_h=100°C, T_e=6°C, t=40 min; (4) T_h=110°C, T_e=6°C, t=40 min. Various methods have been used to control the evaporation temperature and heat source temperature properly. The cooling power is evaluated by the averaged temperature difference of inlet and outlet of chilled water in the evaporator multiplied by the mass flow rate of the chilled water and the specific heat of water. The COP of the system is evaluated as the cooling capacity divided by the heat input, in which the heat input is counted by an electric kW·h counter.

Modifications regarding to the heat dissipation of the heating line and boiler to the environment and the heat leak to the evaporator were carried out by experiment, further calculation regarding the difference of heat capacity of thermal fluid between oil and water were also performed (currently water was used as thermal fluid, however oil is the real reasonable fluid for the system). The real system performances with respect to the above four operation conditions are shown in Table 7. Table 8 shows the predicted performance of the system based upon experimental results.

The above operation is not completely ideal, heat recovery is effective only for sensible heat, mass recovery have been adopted and was found effective. The further improvement is the heat recovery of adsorption heat. By the way it was observed

Table 7
Concluded performances of the adsorption heat pump with respect to four operation conditions[a]

T_h (°C)	t (min)	T_d (°C)	T_a (°C)	T_c (°C)	T_e (°C)	Q_f (kW)	SCP_2 (W/kg)	SCP_1 (W/kg)	COP	No.
100	50	98.7	46.9	24.0	9.6	3.80	146	159	0.4	1
100	40	96.8	45.6	29.6	9.9	3.93	151	168	0.37	2
100	40	97.8	44.2	26.8	6.1	3.46	133	148	0.34	3
110	40	106	45.7	28.7	6.0	3.70	143	159	0.32	4

[a] Q_f, averaged refrigeration power; SCP_1, adsorption pair specific cooling power; SCP_2, system specific cooling power.

Table 8
Several measured performances and its prediction after improving insulation and substituting heat medium (water to oil) [15]

Performances	Operation condition No. 1	No. 2	No. 3	No. 4
SCP_{water}	159	168	148	159
COP_{water}	0.40	0.37	0.34	0.32
$SCP_{water, true}$	166	171	151	161
$COP_{water, true}$	0.43	0.40	0.37	0.34
$SCP_{oil, true}$	166	171	151	161
$COP_{oil, true}$	0.50	0.47	0.44	0.39

that thermal conductivity in the bed is very critical, the heat of adsorption was not transferred effectively, the adsorption temperature was about 45°C, which is still very high. If the effective heat transfer coefficient in the adsorber was increased, the system performances will be improved significantly.

The reversed operation for heating with the adsorption heat pump was carried out, and found very attractive. In the winter time, when the environmental temperature is about 0–10°C, and the temperature lift is about 20–30°C, the system heat pumping efficiency COA=1.3–1.5, while the specific heating power SHP=280–500 W/adsorber kg-adsorbent. Table 9 shows some experimental results.

Table 9
Adsorption heat pump performance for heating in winter time

Cycle time (min)	Heat source temp. (°C)	Heat pump power (kW)	COA	Heating temp. (°C)	SHP (W/kg)
30	7.21	12.669	1.47	37.92	487
40	9.18	9.946	1.41	33.49	382
50	6.22	8.28	1.35	28.66	318
60	1.51	7.314	1.33	22.30	281
60	9.76	9.56	1.54	37.93	368

The heat pump research shows that adsorption heat pump is capable of cooling and heating, the heating performance is attractive. It will be of much better performances if the bed thermal conductivity is increased significantly.

10. Current work with the application potentials of adsorption systems

A lot of research regarding to adsorption refrigeration or heat pump systems have been performed in SJTU, the main work now is focused on solar adsorption refrigeration and air conditioning, the waste heat driven adsorption air conditioning for automobiles.

Solar adsorption ice maker seems to be attractive, 5–7 kg ice/day has been achieved with 1 m^2 plate type adsorber as solar collector, in which activated carbon–methanol is adopted. A potential application of solar adsorption refrigeration is for air-conditioning, such as household air conditioning and air conditioning for grain storage. It is expected to use solar plate type adsorber to assure low cost, the expected 1 m^2 adsorber will be less than 100 US$, which will be of commercial interests. With 6–8 m^2 adsorber, it is possible to establish a 20 m^2 room air conditioner, which has a running time of 8 h. The obvious benefits of solar adsorption system is that the solar energy is used for desorption during the day, the adsorption air-conditioning system can be used when needed. In such applications, both zeolite–water and activated carbon–methanol can be used.

Automobile air conditioning driven by the exhausted gas is really very attractive due to the use of natural refrigerants and nearly no energy cost, however it is very difficult. The difficulties are the size of an adsorption air conditioning system is much bigger than a normal electric driven vapor compression system, the cooling supply stability is difficult to control. The research in SJTU now includes (1) adsorption bus air-conditioning with a cooling capacity of about 20 kW, in which activated carbon–ammonia is adopted, continuous operation will be achieved with the operation phase change of two adsorbers, the two adsorbers for 20 kW air conditioning will be constrained in 1 cm^3 space. (2) Adsorption air conditioning system for train locomotive driver with a cooling capacity of 5 kW, in which zeolite–water is adopted. Continuous cooling is achieved by cold storage though only one adsorber is used in the system. This design is based upon simple operation, and easy maintenance. Zeolite–water is of the best performances for adsorption air conditioning driven by the exhausted gas from an engine, its COP can reach 0.4, however reliability is critical as it is operated in vacuum system. Activated carbon–ammonia is of good reliability, but its COP is only half that of zeolite–water. Waste heat recovery and refrigeration capacity should be matched in the design besides the adsorption system itself.

11. Concluding remarks

Various research aspects on adsorption refrigeration have been completed in SJTU, some new researches are still going on. The following Table 10 shows the concluded research achievements regarding adsorption refrigeration in SJTU.

Table 10
Concluded achievements and remarks of adsorption refrigeration research in SJTU

Adsorption systems	Performance details	Remarks
Solar ice maker (activated carbon–methanol)	COP_{solar}=0.11–0.13, 5–7 kg-ice/m^2-solar collector.	Tested
Hybrid solar water heater and ice maker/refrigerator (activated carbon–methanol)	2 m^2 vacuum solar collector yields 60 kg 85–100°C hot water and 5 kg ice, or keep a 120 liter cold box with a temperature lower than 5°C for 50 hours.	Tested
Low temperature waste heat source driven ice maker (activated carbon–methanol)	With a 100°C heat source, 5.2 kg-ice/kg-adsorbent per day per adsorber has been achieved.	Tested
Low temperature heat source driven air conditioning system (activated carbon–methanol)	With a 100°C heat source, COP=0.5 and SCP=150 W/kg-adsorbent for air conditioning has been achieved, COA=1.3–1.5 and SHP=300–500 W/kg-adsorbent for heat pumping has been obtained with a temperature lift about 30°C.	Tested
Bus air conditioning driven the exhausted gases (activated carbon–ammonia)	A 5 kW prototype has been constructed and will be tested soon, a 20 kW system will be designed.	To be tested
Adsorption air conditioning system for train locomotive driver (zeolite–water)	A 5 kW system has been constructed, Continuous cooling is achieved by cold storage though only one adsorber is used in the system.	To be tested
Solar air conditioning (zeolite–water, activated carbon–methanol)	A 8 m^2 solar adsorber, yields 8 h cooling for a 20 m^2 room. Plate type and tube type adsorbers will be tried and tested.	To be tested

The research results show

1. Solar adsorption refrigeration and air-conditioning are reasonable for future application.
2. Waste heat driven adsorption systems should be market-attractive for application in energy utilization systems.
3. Adsorption heat pump for house hold application should be of interests as its COA and SHP are higher.

Acknowledgements

This work was supported by the State Key Fundamental Research Program under the contract No. G2000026309, the Teaching and Research Award Program for Outstanding Young Teachers in Higher Education Institutions of MOE, P.R.C., and Shanghai Commission of Science and Technology. The supports from Carrier Corporation and UTRC are specially appreciated. The author thanks a lot to Dr J.Y.

Wu, Mr Y.X. Xu, Dr M. Li, Dr W. Wang, Mr L.M. Yang, Mr Q.B. Wang, Mr Y.B. Gui, Mr J. Cheng and Dr Y. Teng for their contributions in the research work.

References

[1] Wang RZ, Wang QB. Adsorption mechanism and improvements of adsorption equation for adsorption refrigeration pairs. International Journal of Energy Research 1999;23(10):887–98.
[2] Teng Y, Wang RZ, Wu JY. Study of the fundamentals of adsorption systems. Applied Thermal Engineering 1997;17(4):327–38.
[3] Wang RZ, Wu JY, Xu YX, Wang W. Performance researches and improvements on heat regenerative adsorption refrigerator and heat pump. In: Proceedings of the International Sorption Heat Pump Conference. Germany: Munich, 1999:631–8.
[4] Yang LM, Wang RZ, Wu JY. Study on the thermal wave cycle in the adsorption refrigeration. Journal of Engineering Thermophysics 1997;18(6):673–6 In Chinese.
[5] Shelton SV, Wepfer WJ. Solid-vapor heat pump technology. In: Proceedings of the IEA Heat Pump Conference. Japan: Tokyo, 1990:525–35.
[6] Critoph RE. Forced convective enhancement of adsorption cycles. Heat Recovery Systems and CHP 1994;14(4):343–50.
[7] Cheng J, Wang RZ. Analysis on the solid-sorption cycle with forced convective heat and mass transfer inside absorbent bed. Acta Energiae Solaris Sinica 1998;19(4):437–43.
[8] Critoph RE, Thorpe R. Experimental results from a forced convection adsorption heat pump/air-conditioner. In: Proceedings of the International Sorption Heat Pump Conference. Germany: Munich, 1999:555–9.
[9] Tan ZC, Wang RZ. Research on double effect adsorption refrigeration cycle. Acta Energiae Solaris Sinica 1998;19(2):156–60.
[10] Wang RZ. Study on a four-beds cascade adsorption refrigeration cycle capable of COP over 1.1. In: Proceedings of the 20th International Congress of Refrigeration. Australia: Sydney, 1999.
[11] Wang RZ, Li M, Xu YX, Wu JY. A new hybrid system of solar powered water heater and adsorption ice maker. Solar Energy 2000;68(2):189–95.
[12] Wang RZ, Wu JY, Xu YX, Teng Y, Shi W. Experiment on a continuous heat regenerative adsorption refrigerator using spiral plate heat exchanger as adsorbers. Applied Thermal Engineering 1998;18(1-2):13–23.
[13] Wang RZ, Wu JY, Xu YX. A continuous heat regenerative adsorption refrigerator using spiral plate heat exchanger as adsorbers: improvements. ASME Journal of Solar Energy Engineering 1998;121(1):14–9.
[14] Wang RZ, Xu YX, Wu JY, Wang W. Experiments on heat regenerative adsorption refrigerator and heat pump. International Journal of Energy Research 1998;22:935–41.
[15] Wang RZ, Wu JY, Xu YX, Wang W. Performance researches and improvements on heat regenerative adsorption refrigerator and heat pump. Energy Conversion and Management 2000;42(2):233–49.